J. Membrane Biol. 123, 191–207 (1991)
0022263191001192

The Journal of
Membrane Biology

Conformational Changes in Human Red Cell Membrane Proteins Induced by Sugar Binding

Agnes Janoshazi, Gabriela Kifor, and A.K. Solomon
Biophysical Laboratory, Harvard Medical School, Boston, Massachusetts 02115

Summary. We have previously shown that the human red cell glucose transport protein and the anion exchange protein, band 3, are in close enough contact that information can be transmitted from the glucose transport protein to band 3. The present experiments were designed to show whether information could be transferred in the reverse direction, using changes in tryptophan fluorescence to report on the conformation of the glucose transport protein. To see whether tryptophan fluorescence changes could be attributed to the glucose transport protein, we based our experiments on procedures used by Helgerson and Carruthers [Helgerson, A.L., Carruthers, A., (1987) *J. Biol. Chem.* **262**:5464–5475] to displace cytochalasin B (CB), the specific D-glucose transport inhibitor, from its binding site on the inside face of the glucose transport protein, and we showed that these procedures modified tryptophan fluorescence. Addition of 75 mM maltose, a nontransportable disaccharide which also displaces CB, caused a time-dependent biphasic enhancement of tryptophan fluorescence in fresh red cells, which was modulated by the specific anion exchange inhibitor, DBDS (4,4′-dibenzamido-2,2′-stilbene disulfonate). In a study of nine additional disaccharides, we found that both biphasic kinetics and DBDS effects depended upon specific disaccharide conformation, indicating that these two effects could be attributed to a site sensitive to sugar conformation. Long term (800 sec) experiments revealed that maltose binding (± DBDS) caused a sustained damped anharmonic oscillation extending over the entire 800 sec observation period. Mathematical analysis of the temperature dependence of these oscillations showed that 2 μM DBDS increased the damping term activation energy, 9.5 ± 2.8 kcal mol^{-1} deg^{-1}, by a factor of four to 39.7 ± 5.1 kcal mol^{-1} deg^{-1}, providing strong support for the view that signalling between the glucose transport protein and band 3 goes in both directions.

Key Words red cell · glucose transport protein · band 3 · anion exchange protein · maltose · disaccharides · anion transport inhibitors · DBDS

Introduction

Janoshazi and Solomon (1989) studied interactions among the red cell anion transport protein, band 3, and other membrane transport proteins using, as a probe, the fluorescent stilbene anion transport inhibitor, DBDS (4,4′-dibenzamido-2,2′-stilbene disulfonate), which binds specifically to the anion transport exchange protein, band 3. We concluded that the glucose transport protein (GTP) and band 3 were in contact, either directly or through an intermediate, so that information could be transmitted between these two transport proteins. Our conclusion was supported by a number of experiments with cytochalasin B (CB), which is a specific inhibitor of glucose transport. CB modulates the time course of DBDS binding to band 3 with an ID_{50} virtually the same as the K_D found by Carruthers (1986) for CB binding to the glucose transport site. Helgerson and Carruthers (1987) had shown that intracellular, but not extracellular, glucose displaces CB from its binding site on the inside face of the glucose transport protein; we then found that intracellular, but not extracellular, glucose also modulates the kinetics of DBDS binding in the presence of CB (Janoshazi & Solomon, 1989). Extracellular addition of the impermeable disaccharide, D-maltose, which displaces CB (Helgerson & Carruthers, 1987), also modulates the time course of DBDS binding (Janoshazi & Solomon, 1990).

These experiments showed that substrate-induced changes in the conformation of the glucose transporter altered the conformation of the DBDS binding protein. We reasoned that communication should also go in the opposite direction so that DBDS binding, which Dix et al. (1979) had shown to modulate the conformation of band 3, would also alter the conformation of the glucose transporter. Therefore, we instituted a search for a suitable probe of the glucose transporter conformation and chose tryptophan fluorescence. There are six tryptophan residues in the glucose transporter, of which two are in the bilayer, or adjacent to it, as located in the sequence of Mueckler et al. (1985). Gorga and Lienhard (1982) had previously studied the tryptophan fluorescence of the purified red cell glucose trans-

porter and reported that both CB and D-glucose quenched the fluorescence. Subsequently Carruthers (1986) used tryptophan fluorescence in stripped human red cell ghosts to determine the K_D for D-glucose binding to both inward and outward facing sites. The problem with tryptophan fluorescence measurements arises from possible ambiguities in interpretation due to the tryptophan residues in band 3, although the presence of band 3 in the stripped ghosts used by Carruthers did not interfere with his measurements. However, Verkman et al. (1986) reported that DBDS modulates the time course of tryptophan fluorescence, following addition of the mercurial sulfhydryl reagent, pCMBS (*p*-chloromercuribenzene sulfonate) to white ghosts, in a reaction attributed to band 3. Thus, extensive control experiments are necessary to assign the signal we observe to the glucose transport protein. Dansyl glucosamine, which is a more specific fluorescent probe of the glucose binding sites, is not satisfactory because the ambiguities as to the specific binding locus of this probe are more refractory than the problem of assignment of the tryptophan fluorescence changes.

We found that the nontransportable disaccharide, D-maltose, caused a time-dependent change in tryptophan fluorescence over the very long period of 50–200 sec and that this time course was modulated by 2 μM DBDS in a time-dependent manner. Barnett, Holman and Munday (1973) had found that D-maltose and other disaccharides inhibited sugar transport and that the K_I depended upon disaccharide conformation, thus showing that the extracellular sugar binding site discriminates among the disaccharides. We studied several disaccharides and found that both the kinetics of binding and the effect of DBDS depend upon the conformation of the sugar.

Since the slow time course of the tryptophan kinetics observed subsequent to maltose binding cannot be fit by a sum of exponential terms, the kinetics are not governed by a conventional series of sequential reactions. However, the kinetics can be fit with the equations for a damped anharmonic oscillation, with four adjustable parameters. When the temperature dependence of the parameters describing the damping, $p(2)$, and the angular frequency terms, $p(3)$, are plotted as Arrhenius plots, the activation energies are $p(2)$, 9.5 ± 2.8 and $p(3)$, 7.6 ± 0.9 kcal mol^{-1} deg^{-1} consistent with restraints by H-bonds. When the red cells have been treated with 2 μM DBDS, the $p(2)$ activation energy is increased to 38.9 ± 5.2 kcal mol^{-1} deg^{-1}. This significant increase in the activation energy of the damping term shows quantitatively that the maltose-induced kinetics are modified by DBDS. These data provide the strongest support for our conclusion that the stilbene disulfonic inhibitors cause conformation changes in the glucose transporter and that the signalling between this protein and band 3 goes in both directions.

Materials and Methods

Materials

DBDS, synthesized by the method of Kotaki, Naoi and Yagi (1971) was kindly supplied by Dr. J.A. Dix. DIDS was obtained from Molecular Probes (Junction City, OR). D-glucose, L-glucose, 4,6-O-ethylidene-D-glucose, D-maltose, maltotriose, cellobiose, trehalose, palatinose and lactose were purchased from Aldrich (Milwaukee, WI). Maltitol, sucrose and lactulose were purchased from Sigma (St. Louis, MO). The remaining reagents were purchased from Fisher (Medford, MA) and Sigma.

Methods

Preparation of Blood Cells and Ghosts

Outdated bank blood was kindly supplied by the Children's Hospital (Boston, MA). After aspiration of plasma and buffy coat, the blood was washed three times with PBS buffer of the following composition (mM): NaCl 150; Na_2HPO_4 5, pH 7.4; 300 ± 5 mOsm. Other buffers used in these experiments were as follows: hemolysis buffer, 5 mM Na_2HPO_4, pH 8.0; ghost buffer, 250 mM glucose, 25 mM NaCl, 5 mM Na_2HPO_4, pH 7.4; glucose (or other specified saccharide) buffer, 150 mM saccharide, 75 mM NaCl, 5 mM Na_2HPO_4, pH 7.4. Osmolality was measured by a Fiske Osmometer (Model OS; Uxbridge, MA).

Fresh human blood was drawn into a tube containing 10 USP units of heparin/ml blood and was used either immediately or after storage (no more than 2 days) at 2–4°C. Prior to each experiment the blood was washed three times in PBS (dilution 1 : 40). Between the first and second washes the cells were incubated for 40 min at 37°C to deplete intracellular glucose. After the third wash the cells were diluted 400–500 times and used in the stopped-flow apparatus as described below.

Stripped white ghosts were prepared as described by Carruthers (1986), and used to measure the D- and L-glucose effect on tryptophan fluorescence.

Pink one-step ghosts were made by lysing the washed red cells 1 : 20 in the osmotic lysis solution. After allowing hemolysis to proceed for 5 min, the ghosts were centrifuged at $15{,}000 \times g$ for 10 min and the red pellet was resuspended at $\approx$1 : 5 (vol/vol) in PBS, pH 7.4. One-step ghosts were incubated for 1 hr at 37°C with PBS or ghost buffer to promote resealing and were used for D-glucose influx and efflux experiments.

D-Glucose Influx and Efflux Measurement

D-glucose efflux was measured in pink ghosts prepared as described above from D-glucose depleted washed red cells. The pink ghosts were then resealed in ghost buffer for 1 hr at 37°C. After incubation, D-glucose was washed off from the outside of the membranes with PBS. The washed pink ghosts were resus-

pended in PBS (1 : 100), and tryptophan fluorescence was used to measure the efflux from $t = 0$ until $t = 15$ min. The baseline correction compensated for cell settling.

D-glucose influx was measured in pink ghosts by suspending glucose-depleted pink ghosts, prepared in PBS as described above, in ghost buffer (1 : 100). Influx was measured by tryptophan fluorescence over a 150-sec period (with baseline correction). The shape and the position of the fluorescence emission peak are time independent.

Fluorescence Measurements

Fluorescence measurements were performed (normally at 20–25°C) with a single beam spectrophotometer (Photon Technology International, South Brunswick, NJ), which uses a reference channel quantum counter for signal normalization. The observation cuvette (vol: 400 μl) is part of a temperature controlled stopped-flow apparatus (model SFA-11, Hi-Tech Scientific, Salisbury, UK). The dead-time, which is governed by the software of the data acquisition system supplied with the Photon Technology instrument, is of the order of 100 msec.

Tryptophan fluorescence was measured using 280 nm for excitation (resolution 4 nm) and 332 nm for emission (resolution 4 nm). We used a 280 ± 10 nm bandpass filter in the excitation path to improve the signal. Unless otherwise specified, the data acquisition rate was 3 msec/point. For the steady-state measurements we measured the stability of the tryptophan signal over a 200-sec period and did not find any decay in the fluorescent signal, though a decay ascribed to the photolysis of tryptophan residues was observed by Appleman and Lienhard (1985) under different conditions, in their apparatus which used wider slits. Nonetheless, we corrected our experiments by subtracting the baseline, unless otherwise specified. DBDS fluorescence was measured with excitation, 360 nm (resolution, 5 nm); emission, 430 nm (resolution, 4 nm). We used a 360-nm bandpass filter for excitation, and for emission a 421-nm cut-off filter. To measure light-scattering in the D-glucose uptake experiment, we measured emission at 430 nm (resolution 4 nm) and placed a 410-nm cut-off filter in the emission light path. The amplitude of the 430-nm signal is an order of magnitude smaller than the tryptophan fluorescence signal.

Binding of Maltose and Other Disaccharides

Unless otherwise specified, these studies were carried out on fresh red blood cells in experiments in which cell suspensions containing 0.2–0.25% washed red cells in PBS were mixed in the stopped-flow apparatus with an equal volume of maltose (or other disaccharide) buffer. The NaCl concentration was adjusted to keep the total osmolality at 310 mOsm in these experiments, as well as in others in which maltose (or other disaccharide) concentrations were varied. Maltose-induced kinetics were measured by tryptophan fluorescence. Unless otherwise specified, experiments were carried out at room temperature, 20–25°C; when the temperature was adjusted to other values, 10 min was allowed for the apparatus to re-equilibrate. In order to maximize the signal/noise ratio, 10–20 runs were averaged, unless otherwise specified.

In order to show that changes in osmotic pressure had no effect on tryptophan fluorescence, we performed a series of experiments in which the NaCl concentration (in 5 mM Na_2HPO_4, pH 7.4) was modified to produce final osmolalities after mixing of: 223, 278, 298, 306 and 349 mOsm. We could not detect any change in the tryptophan fluorescence over a 200-sec period.

To check the reversibility of maltose binding we measured the binding kinetics in a standard experiment with 75 mM maltose. We then washed the mixed solution three times with PBS to make maltose free red cells and once again measured the maltose binding kinetics in a standard experiment. We did not find any difference in the maltose binding kinetics.

Results

Experiments with D-Glucose and 4,6-O-Ethylidene-D-Glucose

We have previously shown that the kinetics of DBDS binding to band 3 depend upon the environment of the transport protein, being significantly different in white ghosts, one-step pink ghosts and red cells (Janoshazi & Solomon, 1989). In order to see whether glucose-induced tryptophan fluorescence also depended upon environment, we compared results in one-step ghosts with those in fresh red cells. Fluorescence was enhanced in both cases: by a factor of 1.07 ± 0.01 in one-step ghosts (3 expts, each an average of 6 runs), as compared to 1.45 ± 0.02 in fresh red cells (6 expts, each an average of 20 runs). These differences show that the properties of the glucose-induced tryptophan fluorescence also depend sensitively upon the environment of the glucose transport protein.

Carruthers (1986) had found that D-glucose *quenches* tryptophan fluorescence by about 10% in his stripped ghost preparation, after correction for nonspecific effects induced by L-glucose, similar to Gorga and Lienhard's (1982) observation that D-glucose binding quenched tryptophan fluorescence in vesicles reconstituted with purified glucose transport protein. In contrast, our experiments in fresh red cells show that D-glucose *enhances* tryptophan fluorescence. In order to determine whether this difference was due to differences in the environment of the glucose transport protein, we carried out control experiments with stripped red cell ghosts, prepared as described by Carruthers. Figure 1 shows the wavelength dependence of fluorescence *quenching* by D-glucose (after allowance for the nonspecific effects produced by L-glucose) which agrees with Carruthers' observations (1986). These experiments show not only that the conformation of the protein depends upon its environment, but also that successful restoration of protein function by reconstitution does not necessarily mean that the protein has regained its native configuration.

Since Krupka (1971) had shown that the glucose transporter conformation changed when extracellu-

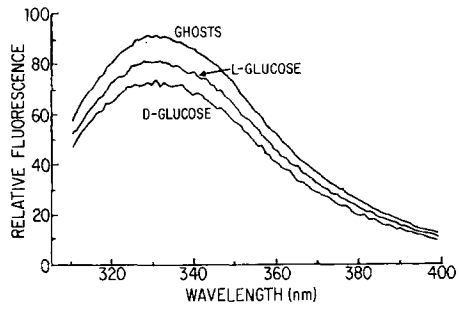

Fig. 1. Emission spectra of stripped red cell ghosts in PBS (0.05 mg/ml protein) with or without 75 mM D- or L-glucose added 15 min before measurements. Average of 10 runs.

lar transportable sugars were bound (*see also* Widdas, 1988) we expected that the course of glucose transport could be followed by tryptophan fluorescence and found this to be so, as shown in Fig. 2*A* and *B*. These experiments were carried out under conditions in which the extracellular glucose concentration remains constant (set at 0 or 250 mM) since the ghosts comprise only 1.0% of the mixed suspension. The data have been fit empirically to single exponentials with time constants of 16.8 ± 1.5 min for influx into glucose-free pink ghosts (Fig. 2*A*) and 3.0 ± 0.8 min for efflux from 250 mM glucose-loaded pink ghosts (Fig. 2*B*) into 0 extracellular glucose. LeFevre (1948) had long ago shown that D-glucose concentrations in the 50–300 mM range inhibit glucose influx; the higher the concentration, the greater the inhibition, so that our time courses measured at 250 mM glucose should be much longer than those measured in the 0–5 mM range. Although LeFevre's data were not fitted to theoretical curves, the half-time for uptake at 50 mM glucose was about 3 min, and that at 0.15 M was many times longer; it was far from its asymptote at 15 min, the end of his experiment, so that our τ of 16.8 ± 1.5 min at 250 mM glucose appears to be in reasonable agreement with LeFevre's data.

To show that the tryptophan fluorescence enhancement following glucose uptake is not to be attributed to increased light scattering, which has long been used to measure glucose-induced volume changes, we measured light scattering at 430 nm to compare with the tryptophan fluorescence at 332 nm. The comparison between these wavelengths in Fig. 2*C* shows that the contribution of volume-induced light scattering is negligible compared to the tryptophan fluorescence enhancement.

Since the extracellular concentrations were time independent in both influx and efflux experiments, the observed change in fluorescence must be attributed to the *intra*cellular glucose level. In the crystallographic analysis of the *E. coli* D-galactose (and D-glucose) binding protein (GBP) one tryptophan residue (GBP Trp 183) is stacked directly below the sugar binding site (Vyas, Vyas & Quiocho, 1988). In the human red cell glucose binding protein, this tryptophan may be analogous to one of the three residues, Trp 363, Trp 388 or Trp 412, in helices 10 and 11 which Walmsley (1988) places in the vicinity of the substrate binding site.

The experiments of Helgerson and Carruthers (1987) provided the basis for a series of control experiments. They showed that *extra*cellular 4,6-O-ethylidene-D-glucose, a nontransportable sugar, displaces CB from its intracellular site on the transporter, though *extra*cellular D- and L-glucose are without effect. As D-glucose enters the cell, CB is displaced with a time course set by the rate of glucose permeation. Our experiments in Fig. 3*A* show that the tryptophan fluorescence enhancement induced at zero time by extracellular addition of 75 mM D-glucose is the same as that induced by its nontransportable analog, L-glucose. As D-glucose permeates the red cell over the next 200 sec, tryptophan fluorescence is significantly enhanced, as compared to the effect of L-glucose. In another control experiment, we found that 2 μM CB inhibits D-glucose uptake (*data not shown*). 75 mM 4,6-O-ethylidene-D-glucose quenches the fluorescence substantially (Fig. 3*B*), similar to the effect observed by Gorga and Lienhard (1982) on the isolated transport protein. Alvarez et al. (1987) have shown that 4,6-O-ethylidene-D-glucose causes a change in the conformation of the reconstituted red cell glucose transport protein, as measured by Fourier transform infrared spectrometry. Thus, the conformation changes at the intracellular transport site which lead to CB release are correlated with tryptophan fluorescence changes. Since intracellular D-glucose (Fig. 3*A*) and extracellular 4,6-O-ethylidene-D-glucose (Fig. 3*B*) exercise opposite effects on tryptophan fluorescence, it is clear that they cause different conformation changes, which is not unexpected since the actions are initiated on different faces of the cell membrane.

Experiments with D-Maltose

Kinetics

The nontransportable disaccharide, D-maltose, which inhibits glucose transport, binds to the outside face of ghosts with K_d = 0.9 to 2.9 mM (Helgerson & Carruthers, 1987; Carruthers, 1986) and displaces

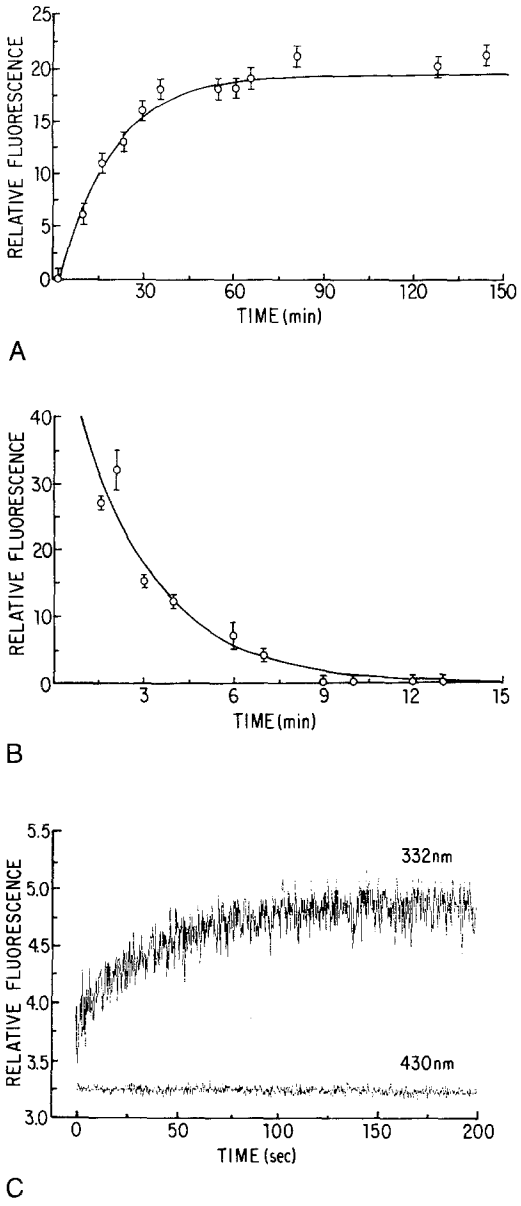

Fig. 2. (*A*) D-glucose influx measured by tryptophan fluorescence. Pink ghosts resealed in PBS were resuspended to 1% in ghost buffer and placed in a microcuvette whose fluorescence intensity was measured at appropriate intervals after suspension. The position and shape of the emission peak did not change over the course of the influx and efflux measurements. Each point is the average of 10 measurements; data were corrected for cell settling and fit empirically to a single exponential by nonlinear least squares. τ_{influx} = 16.8 ± 1.5 min. One expt of two. (*B*) D-glucose efflux in pink ghosts, measured by tryptophan fluorescence intensity. Ghosts were resealed in ghost buffer for 1 hr at 37°C and then washed twice (quickly) in cold PBS (5°C) and resuspended in PBS buffer (1% suspension; 0 glucose). Measurements and data fitting as in *A*. τ_{efflux} = 3.0 ± 0.8 min. One expt of two. (*C*) D-glucose influx in red cells, measured at two different emission wavelengths (excitation, 280 nm; emission, 332 (tryptophan) or 430 nm; resolution, 4 nm). Red cells in PBS (0.2% solution) were mixed in the stopped-flow apparatus with an equal volume of D-glucose buffer. Average of 4 runs for tryptophan signal; average of 26 runs for 430 nm signal. The intensity of the 332 nm peak was 30,000 ± 1000 fluorescence units, an order of magnitude greater than the intensity of the 430 nm peak, 2700 ± 90 fluorescence units. Curves have been shifted for visibility.

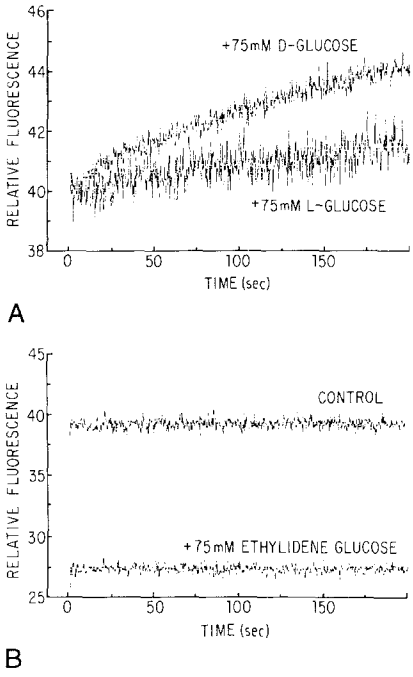

Fig. 3. (*A*) Tryptophan fluorescence in red cells after starvation for 1 hr at 37°C and one wash in PBS. Cells resuspended in PBS at 0.25% were mixed with equal volumes of D- or L-glucose buffer. Baseline corrected; average of five measurements per experiment. One of three expts. (*B*) Effect of 75 mM 4,6-O-ethylidene-D-glucose on tryptophan fluorescence of starved red cells, measured as in *A*. For the control an 0.25% suspension of red cells in PBS were mixed with an equal volume of PBS. One of two expts.

CB from its binding site on the inside-facing carrier. The control experiment in Fig. 4*A* shows that maltose inhibition of D-glucose transport can also be observed by tryptophan fluorescence enhancement. We have also found that D-maltose binding produces a time and concentration-dependent enhancement of tryptophan fluorescence. The time course at 65 mM D-maltose, shown in Fig. 4*B*, consists of a rapid enhancement step (phase 1), too fast for us to resolve, followed by a slowly rising phase of about 75–150 sec (phase 2) and a subsequent slow biphasic decrease in signal for the next 50–100 sec (phase 3). As D-maltose concentration increases, as shown in Fig. 4*B*, the slope of phase 2 increases and the onset of phase 3 takes place sooner, so the transition between phases 2 and 3 is concentration dependent. Since Fig. 4*B* shows that the amplitude of the initial step, phase 1, is also concentration dependent, the

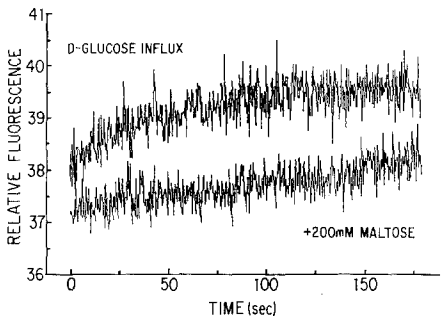

A

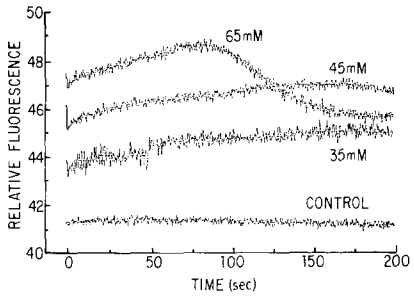

B

Fig. 4. (*A*) Effect of 200 mM maltose on D-glucose influx at 20–25°C. A 0.2% suspension of D-glucose-free red cells in 200 mM maltose, 45 mM NaCl, 5 mM Na_2HPO_4, pH 7.4, was mixed with an equal volume of solution containing 100 mM D-glucose plus 200 mM maltose (bottom trace). In the top trace, a 0.2% suspension of D-glucose-free red cells in PBS was mixed with an equal volume of 100 mM D-glucose, 98 mM NaCl, 5 mM Na_2HPO_4, pH 7.4. The osmotic pressure was maintained at 306 mOsm in both solutions. (*B*) Concentration dependence of D-maltose induced tryptophan fluorescence kinetics at 20–25°C. An 0.2% red cell suspension in PBS was mixed with maltose buffer (adjusted to appropriate maltose concentration with osmolality maintained at 310 mOsm by adjustment of [NaCl]); baseline corrected. 15 runs averaged for each curve; data for one of three experiments on different bloods.

entire reaction sequence depends upon D-maltose binding and all three phases appear to be part of a coupled sequence, driven by the chemical concentration of D-maltose.

The difference between fresh red cells and washed ghosts observed with glucose binding extends to D-maltose binding as well, since D-maltose binding in stripped white ghosts produces a small fluorescence quenching, with no evidence of any binding kinetics. Control experiments indicate that the kinetic effects of 75 mM D-maltose binding to red cells are entirely reversible (*see* Methods).

Typically in enzyme-substrate reactions, the initial bimolecular association is followed by a monomolecular rearrangement with an exponential time course such as that which might be represented by phase 2. Thus, if the data stopped at the end of phase 2, phases 1 and 2 might appear to be a conventional enzyme-substrate reaction with an unusually long time constant for the rearrangement. Since the time course doesn't stop there, there must be a subsequent process, possibly a second monomolecular rearrangement, or possibly a dissociation. Either of these reaction steps would have an exponential time course, so that the entire time course of both phase 2 and phase 3 would be described as the sum of two exponentials. We have been unable to fit the time course subsequent to the initial jump by any combination of two exponentials in a five-parameter fit. Therefore, the kinetics are more complex than a sequence of two conventional chemical reactions. Although we would not be able to assign any physical significance to a solution with more than five adjustable parameters, we tried to fit the data empirically with the addition of still another exponential term and even inserted an induction period before the advent of one or both of the phases. Even with these additional degrees of freedom, no fit was possible, so we conclude that the data cannot be described in terms of a circumscribed set of conventional sequential reactions.

The time courses of both phase 2 and phase 3 are measured in tens of seconds, which is very much slower than the conformational changes associated with transport proteins. For example, DBDS binding to band 3 consists of a fast bimolecular association, followed by a conformational change with a time constant of 4 sec^{-1} (Verkman, Dix & Solomon, 1983). Thus the time course of the events subsequent to D-maltose binding further differentiates the process from a conventional chemical binding reaction.

As a consequence, the kinetic data in the following sections[1] are described in general terms and the differences in behavior that we have found are expressed qualitatively and not quantitatively. The time course we observe is a phenomenological description of changes in the environment of the tryptophan residues in the red cell. Any process that changes this environment affects the conformation of the proteins that contain these residues. Insofar as the strategies that we have used to confine our attention to the tryptophan residues in the glucose transport protein are successful, the kinetics we observe can be assigned to changes in the conformation

[1] It will be shown in the final section of the paper and Appendix II that the unusual kinetics probably arise from a damped anharmonic oscillation whose parameters can be obtained in experiments lasting for 600 seconds or more. Since all but the final series of experiments, which allowed us to characterize the oscillations, were carried out for 200 sec, we have not been able to determine the four parameters required for a quantitative analysis of the oscillations in these earlier experiments, which have been analyzed as described in this section of the paper.

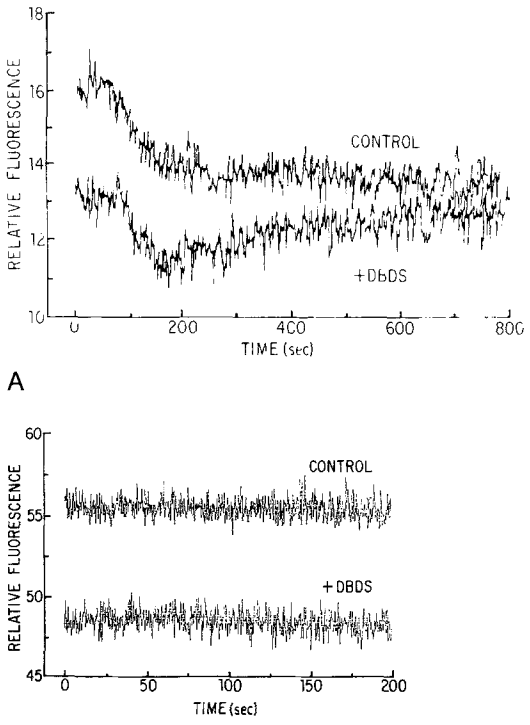

Fig. 5. (*A*) Effect of 2 μM DBDS on D-maltose (75 mM) induced kinetics in red cells over 800 sec. Fresh red cells in PBS (0.2% suspension) were mixed in the stopped-flow apparatus with maltose buffer. Cells were incubated with DBDS for 5 min at 20–25°C. Average of 7 runs. (*B*) Effect of 2 μM DBDS on tryptophan fluorescence in fresh red cells in the absence of D-maltose over 200 sec. Control was red cells (0.2% suspension in PBS) mixed with PBS. Average of 5 runs. Other experiments (*data not shown*) show that these data remain unchanged up to 800 sec.

of the glucose transport protein, independent of the nature of the chemical or physical reactions responsible.

DBDS Effect

When fresh red cells are treated with 2–4 μM DBDS, the D-maltose-induced fluorescence is quenched, as shown in Fig. 5*A*. Observations over 800 sec, clearly show that the difference (± DBDS) decreases with time, so that the DBDS effect is not a simple time-independent displacement and cannot be ascribed either to nonspecific DBDS adsorption to an unrelated site, to nonspecific absorption to the glucose transport protein, or to fluorescence absorption by DBDS. Figure 5*B* shows that the effect of DBDS binding to band 3 in the absence of D-maltose is a simple 20% quenching with no kinetic component,

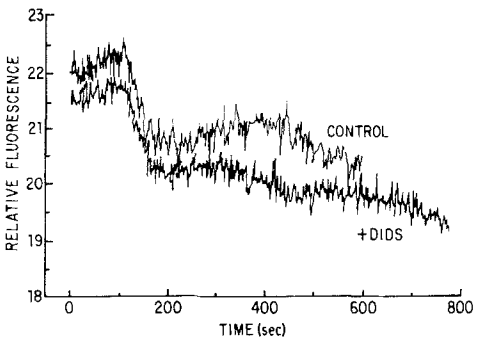

Fig. 6. DIDS modulation of maltose-induced tryptophan fluorescence in fresh red cells. Red cells incubated with 1 μM DIDS for 30 min at room temperature. Otherwise as in Fig. 5*A*.

from which we conclude that D-maltose is essential for the time-dependent changes caused by DBDS (Fig. 5*A*).

The control experiment with DIDS (4,4′-diisothiocyano-2,2′-stilbene disulfonate) in Fig. 6 shows that DIDS also produces an effect on the D-maltose induced kinetics, though in this case the displacement increases with time (from 200 to 400 sec) rather than decreasing, as it does for DBDS. This difference may be ascribed to the fact that DIDS is irreversibly bound to band 3, or it may be ascribed to the fact that the two bulky benzamido substituents at either end of the DBDS molecule are much larger than the isothiocyano substituents at either end of the DIDS molecule. In any case, the effect of stilbene inhibitor binding depends upon the specific conformation of the probe, indicating that the site of the DBDS binding is the stilbene binding site on band 3. Thus, these experiments provide further confirmation of Janoshazi and Solomon's (1989) finding that the glucose transport protein is linked, directly or indirectly, to band 3. Since both the D-maltose and the DBDS binding sites are on the extracellular face of the red cell, it is tempting to think that the extracellular projections of the two proteins are adjacent to one another.

The maltosyl(and lactosyl)isothiocyanate experiments of Rees, Gliemann and Holman (1987) and May (1987) [denoted as hexosylisothiocyanates (HITC)] provide very strong evidence that this is the case, in papers that advance beyond the original HITC experiments of Mullins and Langdon (1980*a*,*b*). Briefly, these papers show that HITC binds to the GTP by finding that HITCs compete for binding with D-glucose and maltose, which are known to bind to the GTP; moreover, L-glucose and sucrose, which have no effect on glucose transport,

also have no effect on HITC binding. The specific inhibitor of glucose transport, cytochalasin B, inhibits HITC binding, and, conversely, HITC binding inhibits binding of cytochalasin B. Taken together, these experiments show that the HITCs bind[2] to the GTP. The isothiocyanate moiety of the HITCs reacts covalently with red cell membrane proteins and gel scans prove that the covalent reaction site is on band 3. Rees et al. (1987) conclude that membrane transport through the GTP can be perturbed by HITC interaction with band 3, and May (1987) suggests that relatively high concentrations of inhibitor acting with one carrier could induce a conformational change in the other, a conclusion for which our experiments provide further support.

Experiments with Other Disaccharides

The biphasic kinetics of the D-maltose-induced tryptophan fluorescence enhancement are characteristic of disaccharide binding and are not found in experiments with monosaccharides. In order to show that the effect is specific to the D-maltose binding site, we have studied several other disaccharides, not only to confirm the specificity of the D-maltose site, but also to give us further information about the sugar substituents which determine the DBDS effect.

Kahlenberg and Dolansky (1972) determined the effect of individual H-bonding sites on the affinity of D-glucose binding to the external site in the red cell by systematic substitution of the glucose hydroxyls. They concluded that H-bonding to the hydroxyls at carbons 1, 3 and 4 of D-glucose and the pyranose ring oxygen were the most important determinants of the binding process and suggested that all the hydroxyls might play a role. Steric factors were also important since the binding site was apparently unable to accept a phenyl group at the C-1 hydroxyl and bulky substituents at C-5 also interfered with binding.

Barnett et al. (1973) subsequently studied the structural requirements for binding to the glucose transport protein by measuring the inhibition constants for competitors of sorbose uptake. Since these were uptake experiments, the results were interpreted as indicative of competition at the extracellular site; indeed, many of the inhibitors were nontransportable sugars. Their results are in general agreement with those of Kahlenberg and Dolansky (1972) in showing the importance of H-bonding at C-1, C-3 and C-4. Barnett et al. (1973, 1975) point out that bulky substituents can be accommodated at C-4 and C-6 and suggest that both C-4 and C-6 are readily accessible from the solution, whereas the other carbons are in close apposition to the site. Both groups of investigators show the glucose molecule in a pocket in the binding site with C-6 pointing out into solution, though other details differ. Such pockets provide a ready mechanism for an oscillating transporter, with D-glucose entering the pocket from one face, followed by closing of the aperture behind the D-glucose and subsequent opening and release on the other side.

The crystallographic studies of Quiocho and his colleagues (Miller et al., 1983; Quiocho, 1986, Vyas et al., 1988) on the sugar-binding proteins in the periplasmic space in *E. coli* provide a framework in which these earlier studies can be incorporated. These investigators have obtained detailed high-resolution studies of the galactose-binding protein (GBP), which also binds D-glucose, the maltose binding protein (MBP) and the arabinose binding protein (ABP). Characteristically, these proteins have a bi-lobed shape, with two globular domains bound together by a hinge composed of three separate protein segments. The binding site for the sugar is located deep inside the cleft, and the first step of binding is a bimolecular association to the site. This is followed by a conformational change in which the two lobes close around the sugar, forcing water out of the cleft and enclosing the sugar in a largely nonpolar environment. The sugars are bound very tightly; for example, D-glucose binds to GBP with $K_D = 0.2\ \mu M$ and D-maltose binds to MBP with $K_D = 35\ \mu M$. Every OH in the sugar is bound to the protein, often multiply by a diverse family of H-bonds. When the lobes close around the embedded sugar, the binding is strengthened further by van der Waal's interactions with aromatic residues, such as tryptophan, positioned above and below the plane of the sugar. GBP is a soluble protein situated in the periplasmic space, with separate sites responsible for both chemotaxis and sugar transport. The periplasmic proteins interact directly with the mem-

[2] The experiments of Rees et al. (1987) showing that D-maltose isothiocyanate (MITC) does not protect the GTP site from interaction with the photoreactive mannose derivative, ASA-BMPA (2-N-(4-azidosalicoyl)-1,3-bis-(D-mannos-4′-yloxy)-2-propylamine), might be interpreted as contrary to this conclusion, but this is not the case. The impermeant ASA-BMPA first binds reversibly, and with high affinity, to the sugar-binding site on GTP; ASA-BMPA is subsequently covalently locked into this GTP-binding site by photoactivation. The maltose moiety of MITC binds reversibly to the sugar-binding site on GTP and the isothiocyanate binds covalently to band 3. Since ASA-BMPA is bound covalently to the sugar-binding site on GTP it can displace MITC which is bound reversibly to the sugar-binding site, notwithstanding the covalent binding of the isothiocyanate moiety of MITC to the adjacent protein, band 3. Thus MITC is unable to protect the sugar-binding site from reaction with ASA-BMPA.

Table 1. Kinetic effects of sugars

	1st sugar	2nd sugar	Biphasic kinetics	DBDS effect
1 : 4 linkage				
-D-pyranosyl (α)				
Maltose	gluco	-D-glucose	yes	yes
Maltotriose	gluco	-D-glucose . . .	yes	yes
Maltitol	gluco	alcohol	yes	yes
-D-pyranosyl (β)				
Cellobiose	gluco	-D-glucose	yes	yes
Lactose	galacto	-D-glucose	yes	yes
Lactulose	galacto	-D-fructose	yes	yes
1 : 2 linkage (β)				
-D-furanosyl				
Sucrose	gluco	-D-fructose	yes	no
1 : 6 linkage (α)				
-D-pyranosyl				
Palatinose	gluco	-D-fructose	yes	no
Melibiose	galacto	-D-glucose	yes	yes
1 : 1 linkage (α)				
-D-pyranosyl				
Trehalose	gluco	-D-glucose	strange	no

brane proteins for onward transport across the inner (cytoplasmic) membrane (*see* Miller et al., 1983). The binding site of MBP discriminates against D-glucose, but binds oligosaccharides as large as maltoheptaose, though MBP is capable of recognizing only three (possibly four) glucosyl units, some parts of which are exposed.

Quiocho (1986) points out that bilobal structures comprise a large proportion of carbohydrate binding proteins and gives several examples of conformational changes that follow apposition of the two domains around the sugar. The features that characterize both the GBP and the MBP fit well with the characteristics of the glucose binding site worked out by Kahlenberg and Dolansky (1972) and Barnett et al. (1973). The arabinose-binding protein, whose structure is similar to the *E. coli* GBP and MBP has been sequenced and found to have homologous ranges, both in sequence and hydropathy analysis, to the red cell glucose transport protein (Mueckler, 1989). These similarities between the red cell glucose transport protein and the *E. coli* sugar binding proteins are particularly compelling and leave little doubt that H-bonding and a shaped cavity are important determinants of disaccharide binding.

In the absence of a kinetic description of the binding and conformational change reactions, it is not possible to express the differences between disaccharides in terms of specific binding constants. Instead we have described the consequences of disaccharide binding in qualitative terms in Table 1 in which the saccharides are grouped according to the linkage between the sugars (*see* Appendix I for structures reproduced from the Merck index). In the section that follows we will give the arguments that lead us to conclude that the biphasic kinetics that we observe result from disaccharide binding to the glucose binding site and that this binding process is modulated by DBDS binding to band 3.

We have adopted the following set of conventions in order to draw conclusions about the molecular configurations and the hydrogen bonds responsible separately for the biphasic kinetics and the DBDS effect:

1. We have arbitrarily denoted the left-hand sugar (as reproduced in Appendix I) as the sugar which binds to the primary binding site in the glucose binding protein (in order to make a construct with which to compare the actions of the various disaccharides). In the case of maltose, this is the -D-glucopyranosyl moiety and it is a -D-pyranosyl moiety in all of the disaccharides we have used (-D-pyranoside in sucrose, which is a -D-furanosyl sugar).

2. We have denoted the glycoside linkages between these monosaccharides as i:j linkages in which i is the C-i- of the left-hand sugar and j of the right hand sugar. Thus maltose (4-O-α-D-glucopy-

ranosyl-D-glucose) is denoted as a 1:4 linkage. The -O-glycoside linkage of all the disaccharides we have studied starts at C-1.

3. We have used Dreiding stereomodels in order to determine whether the 2nd (right-hand) monosaccharide binds to an adjacent H-bonding site, or sites, on the red cell glucose transport protein. The crystallographic structure of the red cell glucose transport protein has not been determined, and it is impractical and essentially impossible to poll all the putative H-bonding sites to the right-hand monosaccharide. Instead, we have arbitrarily focused on the position of the ring -O- of the 2nd (right-hand) sugar which is locked in either a pyranosyl or furanosyl ring. Keeping the position of the left-hand glucose or galactose constant, we have determined whether the position of the 2nd (right-hand) -O- in the other disaccharides is essentially superposable on the 2nd -O- in maltose. If the disaccharide satisfies the 'superposability criterion,' we conclude that it can bind to the disaccharide site to which maltose binds. Admittedly, this is an arbitrary criterion, but one to which conformity can be tested using the Dreiding stereomodels which are accessible to us.

4. There are local differences between the binding affinities of the red cell glucose transport protein and the *E. coli* GBP as far as interactions with H-bonding partners at specific C's, which means that there is diversity in the family of glucose binding proteins. Although our evidence suggests that the biphasic kinetics and DBDS effects are due to ligand binding to the glucose transport protein, substituents at some C's which are important in D-glucose binding have a smaller effect on disaccharide binding. We ascribe this difference to the fact that we probe the site with disaccharides rather than monosaccharides. Accordingly, we will denote the site responsible for the biphasic kinetics as the 'disaccharide' site.

We have used these four principles to examine and classify the time course of the tryptophan fluorescence using the data given in Table 1 on the 10 sugars we have studied.

1. *1:4 Linkage, α Anomer*

These three molecules (maltose, maltotriose, maltitol) are O-α-D-glucopyranosyl molecules with a 1:4 linkage between the two sugars and an analogous link between the sugar and the alcohol. All three of these ligands to the sugar transport protein show both biphasic kinetics and a DBDS effect similar to that shown in Fig. 5*A* for maltose. We can draw the following conclusions:

a. Since D-glucose does not exhibit either biphasic kinetics or a DBDS effect, these effects depend upon interactions either with a disaccharide or at least with a molecule significantly larger than D-glucose. In order to sense the presence of the 2nd sugar (or the alcohol) the disaccharide site must interact with at least one H-bonding site on the 2nd sugar. One acceptable candidate would be the ring -O- in the 2nd D-glucose in maltose. In maltitol, the analogous site is the terminal -OH group on the short limb of the maltitol chain.

b. The fact that maltotriose produces effects similar to maltose shows that the disaccharide binding site can accommodate ligands longer than disaccharides.

2. *1:4 Linkage, β Anomer*

These three molecules (cellobiose, lactose, lactulose), which are O-β-D-gluco(or galacto)pyranosyl molecules with a 1:4 linkage, all exhibit biphasic kinetics and the DBDS effect. The following conclusions may be drawn:

a. H-bonding to the -OH on C-4 of the 1st sugar is not specific since the disaccharide binding site accepts both the D-glucose and D-galactose epimers. Although all three sugars in this group exhibit both biphasic kinetics and the DBDS effect, the fluorescence enhancement of lactose (galacto) is much less than that of cellobiose (gluco), and in lactulose (galacto) the fluorescence is quenched. The D-glucose site seems to be more sensitive to the galactose/glucose difference, since Kahlenberg and Dolansky (1972) have shown that the K_D of the D-galactose/membrane complex is 90 μM, as compared to 27 μM for the D-glucose/membrane complex.

b. The disaccharide binding site does not discriminate between the α and β anomers of the O-glycoside link between the two sugars, since both the α and β anomers exhibit both biphasic kinetics and the DBDS effect. At first sight, this finding is surprising since the change between the anomers leads to a large alteration in the configuration of the 2nd sugar relative to the 1st. However, this lack of discrimination between anomers is characteristic of sugar binding proteins since Quiocho (1989) reports that neither of the *E. coli* sugar binding proteins, GBP or MBP, distinguish between anomers.

c. Cellobiose differs from maltose only in having a β-O-glycoside linkage between the two monosaccharides rather than an α-O-glycoside linkage. In this case the -O- in the glucose in the 2nd sugar of cellobiose is virtually superposable on the -O- in the 2nd sugar of maltose. Lactose (1st sugar: galactose) differs from cellobiose (1st sugar: glucose) only in this galacto/gluco -OH configuration so that lactose also satisfies the superposability criterion. Lactulose differs from lactose by having fructose in place of

glucose as the 2nd sugar. The -O- in the 2nd sugar ring can be brought close to the 2nd -O- site for maltose, though the fit is not as close as for lactose.

The fact that all three sugars in this group satisfy the superposability criterion is consistent with our observations given in Table 1 that all three exhibit both biphasic kinetics and the DBDS effect.

3. *1 : 2 Linkage, β Anomer*

This molecule, sucrose, differs from maltose in having a 1 : 2 linkage, being a β-anomer and in having a D-fructose as the 2nd sugar in place of D-glucose. These differences mean that the -O- in the 2nd ring of sucrose is so far away from the -O- in the second ring of maltose that sucrose does not satisfy the superposability criterion, consistent with our observation that sucrose does not exhibit a DBDS effect.

4. *1 : 6 Linkage, α Anomer*

These sugars (palatinose and melibiose) are linked in the 1 : 6 configuration which means that the 2nd sugar is displaced one additional bond length from the -O- in the 1st gluco (or galacto) sugar. This change also introduces an additional degree of rotational freedom which permits melibiose to satisfy the superposability criterion, consistent with its exhibition of the DBDS effect. In the case of palatinose, which does not have a DBDS effect, the constraints of the furanose ring mean that palatinose does not strictly satisfy the superposability criterion, though the two -O-'s are relatively close. In the case of both melibiose and palatinose, the plane of the 2nd sugar is nearly perpendicular to the 2nd sugar in maltose. These considerations lead us to think that though the superposability criterion may be necessary, it is not sufficient to define those characteristics of the disaccharide site required for the DBDS effect.

5. *1 : 1 Linkage, α Anomer*

The 1 : 1 linkage of trehalose means that the 2nd -O- doesn't even come close to the 2nd -O- in maltose, entirely consistent with the fact that trehalose has neither biphasic kinetics nor a DBDS effect. Figure 7 shows how much trehalose binding kinetics differ from those of maltose.

Taken together, the diversity of our observations on these 10 sugars shows that these sugars bind to a site that discriminates among them according to their detailed molecular configuration, based on the specificity of sugar H-bonding sites. We conclude that the disaccharide binding site incorporates the

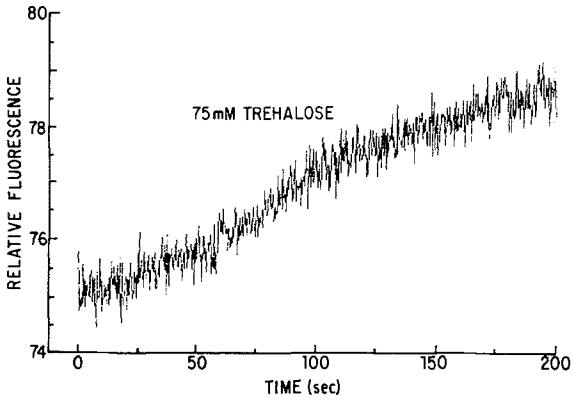

Fig. 7. Trehalose-induced tryptophan fluorescence. Fresh red cells in PBS (0.2% suspension) were mixed in the stopped-flow apparatus with trehalose buffer. Otherwise as in Fig. 5*A*. One expt. of three; average of ten runs per expt.

D-glucose binding site, consistent with the body of physiological evidence showing that extracellular maltose modulates the intracellular configuration of the glucose transport protein (Helgerson & Carruthers, 1987). The disaccharide binding site incorporates at least one additional putative H-bond beyond those that bind D-glucose, which possibly bonds to the ring -O- of the second sugar. At least a single H-bond is necessary, but others probably also come into play, as do steric requirements of the surface, or cavity, to which the disaccharide binds. Our results show that the specific anion transport inhibitor, DBDS, modulates the binding kinetics of selected disaccharides, providing further evidence that conformational information can be transmitted from band 3 to the glucose transport protein.

Oscillatory Nature of Disaccharide Binding Process

When we went through the exercise of trying to accommodate the disaccharide binding kinetics to a conventional reaction scheme, we observed that the time course looked very much like a damped oscillation. In order to see whether the oscillations were real and sustained, we extended some experiments to longer times and detected traces of a damped oscillation extending out to 12 min, as shown in Fig. 8*A*. In view of the very long period of these oscillations and the unusual nature of our finding, we carried out a number of experiments trying to relate the oscillations to a physical cause. Since red cell cation fluxes are slow, and since K^+ flux can be mediated by Ca^{2+} we incubated the cells with the ionophore, A23187, for 20 min to remove all the

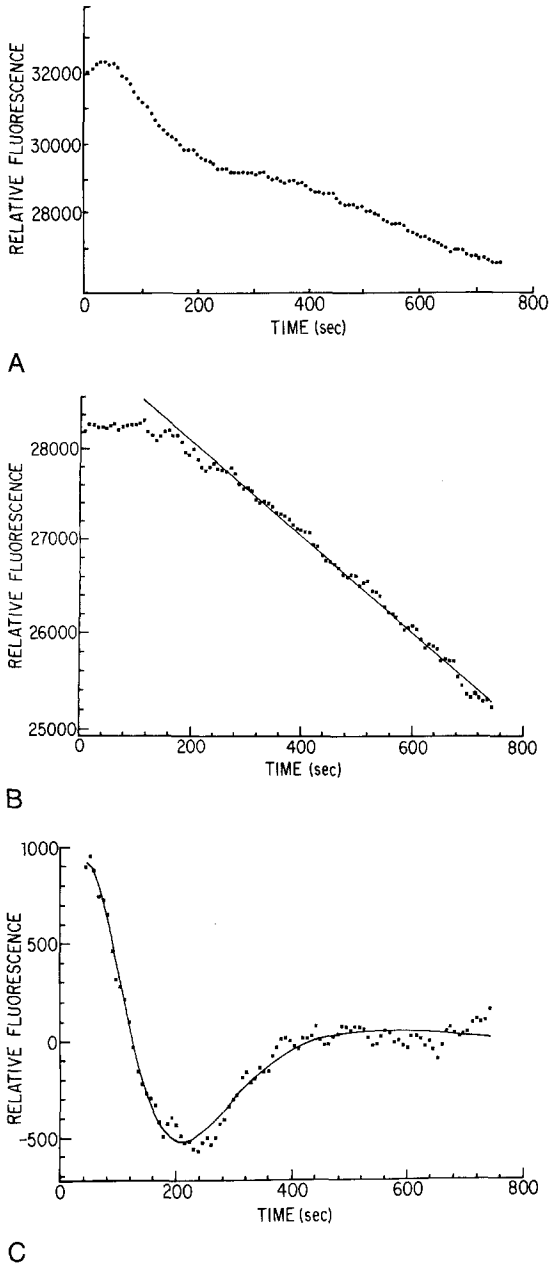

Fig. 8. Method for correcting data for baseline shift and fitting to damped anharmonic oscillation model. (*A*) Raw data of 75 mM maltose induced tryptophan fluorescence kinetics (0.2% suspension, before mixing) over 12 min period. Data obtained as in Fig. 5*A*. (*B*) Baseline drift measured under same conditions as Fig. 8*A*, except the mixing solution was PBS (0 maltose). The baseline, which remains approximately constant for the first 200 sec and then falls exponentially, has been fitted by nonlinear least squares to the exponential $p(5)\exp[-p(6)t]$ with $p(5) = 0.29 \pm 0.01 \times 10^5$ fluorescence units and $p(6) = 0.19 \pm 0.04 \times 10^{-3}$ sec^{-1}; the fitted line is shown. (*C*) The data in Fig. 8*A* were fitted by nonlinear least squares to the six parameter equation (Appendix II Eq. (A7) with the parameters: $p(1) = 1100 \pm 90$ fluorescence units; $p(2) = 0.0032 \pm 0.0004$ sec^{-1}; $p(3) = 0.029 \pm 0.006$ sec^{-1}; $p(4) = 8.5 \pm 1.1$ sec; $p(5) = 0.32 \pm 0.11 \times 10^5$ fluorescence units and $p(6) = 0.24 \pm 0.03 \times 10^{-3}$ sec^{-1}. The data and the fitted curve have been corrected by subtracting the term in $p(5)$ and $p(6)$ using the parameters determined in the six-parameter fit.

Ca^{2+} and Mg^{2+} from the cells in one experiment; in another, we substituted Na^+ for K^+ in the extracellular buffer. In an additional set of experiments to determine whether Cl^- was important to the oscillations, we substituted gluconate for Cl^- in the buffer. Though these changes sometimes modified the time course of the response and sometimes were without effect, none of them abolished the oscillations. We next examined whether the oscillations might be driven by ATP or the Na^+ or K^+ ion fluxes, so in one experiment, we incubated the red cells with 5 mM iodoacetamide + 5 mM inosine for 3 hr at 37°C to starve the cell of metabolic energy (Lew, 1971), and in another we incubated the cells with 10 mM Na_2SO_3 + 8 mM NaF for 10 min at room temperature (Duhm, Deuticke & Gerlach, 1969). We also altered the Na^+ and K^+ gradients to minimize the cation fluxes. Again, though these treatments sometimes modified the kinetics, none of them abolished the oscillations. We concluded that the oscillatory behavior was independent of metabolic energy and ionic gradients, which sets our findings apart from metabolic energy-dependent biochemical oscillations (*see*, e.g., Chance et al. (1973)).

We were then struck by the crystallographic descriptions of the glucose binding process in *E. coli*, given by Quiocho and his colleagues (Miller et al., 1983, Quiocho, 1986, Vyas et al., 1988). As we have discussed, after the D-glucose molecule binds in the bottom of a deep cleft between two separate lobes of the *E. coli* GBP, the cleft closes around the bound D-glucose, forces out water and strengthens the binding with additional van der Waals forces, including those between the D-glucose and a neighboring tryptophan. The engulfing of the D-glucose produces a conformational shift estimated by Miller et al. (1983) as a 20° rotation in the lobes of the GBP, causing a decrease in the radius of gyration of about 1 Å. We reasoned by analogy that the energy for our oscillations could be provided by the binding force of the disaccharides to the red cell glucose transport protein. As the site snapped shut about the bound disaccharide, the resultant conformational change could initiate the oscillatory process.

The time course of our oscillations is extraordinarily long, even compared to the rate of unbinding of D-glucose from the *E. coli* GBP, which Miller et al. (1983) give as 1.4 sec^{-1}. Such a long period might be rationalized by considering that the glucose transport protein forms a constituent part of the red cell megadalton enzyme/transport complex. Fossel and Solomon (1978) showed that the red cell glycolytic enzymes are bound in a megadalton complex attached to the cytosolic pole of band 3 to which both glyceraldehyde 3-phosphate dehydrogenase (G3PD) and aldolase bind specifically (Yu & Steck, 1975; Strapazon & Steck, 1977); recently Rogalski, Steck

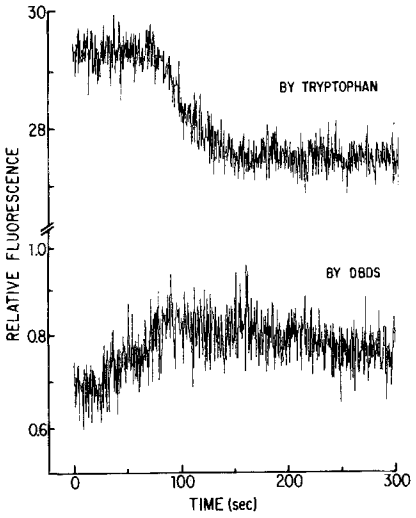

Fig. 9. Effect of D-maltose (75 mM) binding to red cells (0.2%) in the presence of 2 μM DBDS measured either by tryptophan fluorescence (excitation, 280 nm; emission, 332 nm) [top curve] or by DBDS fluorescence (excitation, 360 nm, emission, 430 nm, resolution 4 nm) [bottom curve].

and Waseem (1989) have shown that all of the human red cell G3PD is bound to the membrane. Janoshazi and Solomon (1989) have shown that the red cell Na^+,K^+-ATPase is also bound to band 3, which is itself linked to the cytoskeleton by ankyrin (*see* Bennett & Stenbuck, 1980). Coupling to such a large family of membrane and cytosolic proteins might account for the very long period between successive peaks. If this explanation of a damped oscillation in the metabolic/transport enzyme complex is correct, we would expect to see related conformational changes in other enzymes in the complex. Accordingly, we compared the time course of tryptophan fluorescence with that of DBDS fluorescence, following addition of 75 mM maltose, and obtained the results in Fig. 9. It can be seen that the two time courses are complementary, which means that the conformation changes we have observed in the red cell glucose transport protein are reflected in the configuration of band 3.

In order to get further insight into the energetics of the oscillatory process, we carried out two experiments (at seven temperatures) on the temperature dependence of maltose binding, in the presence and absence of DBDS, and analyzed the results using the model of a classical damped anharmonic oscillator. The following equation, which is derived in Appendix II [Eq. A8), describes the time course of fluorescence enhancement, $y(t)$:

$$y(t) = p(1)\exp[p(2)(t - p(4))]\sin\{(t - p(4))p(3)\exp[p(2)(t - p(4))/2]\}. \quad (1)$$

Table 2. Apparent activation energy for tryptophan oscillations

exp	$p(2)$ (slope) (kcal mol^{-1} deg^{-1})	$p(3)$ (slope) (kcal mol^{-1} deg^{-1})
Blood 1	8.1 ± 0.6	5.9 ± 0.6
Blood 2	10.8 ± 2.7	9.3 ± 0.7
average	9.5 ± 2.8	7.6 ± 0.9
+ DBDS (2 μM, blood 2)	38.9 ± 5.2	10.8 ± 2.8

Though the parameters $p(1)$ . . $p(4)$ are defined exactly in Appendix II, it is helpful to describe them in qualitative terms. $p(1)$ is the amplitude of the oscillation; if the equation were a simple damped harmonic oscillation, $p(2)$ would be the damping and $p(3)$ would be the angular frequency if damping were absent; $p(4)$ is t_o, the time delay before the oscillation begins. In order to exhibit the damped oscillations that we observe, the binding process must be synchronous in all the red cell glucose transport proteins, which is probably easily accomplished since the time constant for maltose binding to the *E. coli* MBP is 2.3×10^7 M^{-1} sec^{-1} (Miller et al., 1983), orders of magnitude faster than the time scale of the oscillations. The attractive forces responsible for the anharmonicity of the oscillations could be attributed to the van der Waals forces that are strengthened when the binding site snaps shut, and the damping of the oscillations could arise from the inhomogeneity of the multiple proteins that may be involved in the enzyme/transport complex. Figure 8, which is discussed fully in Appendix II, shows the raw data in the absence of base line correction (Fig. 8*A*), the base line correction (Fig. 8*B*) and the fitted data (Fig. 8*C*). The fit in Fig. 8*C* shows that the mathematical model in Eq. (1) provides a good fit to the experimental data.

Comparison of the results of the control experiments at 15 and 27°C in Fig. 10*A* and *B* shows clearly that the oscillations are temperature dependent and that the half-width of the first cycle narrows as the temperature rises. The difference between the curves in the presence of 2 μM DBDS provides clear evidence that DBDS modulates the time course of maltose-induced tryptophan fluorescence. DBDS decreases the amplitude of the signal at both temperatures, but the most striking DBDS effect is on the damping of the signal, which is sharply reduced at 15°C, as compared to 27°C.

In order to express the temperature effects quantitatively we have plotted $p(2)$ and $p(3)$, the damping and the angular frequency terms, as Arrhenius plots, as shown in Fig. 11*A* and *B*. Table 2 gives the average activation energy for the damping factor as 9.5 kcal mol^{-1} deg^{-1} and for the angular

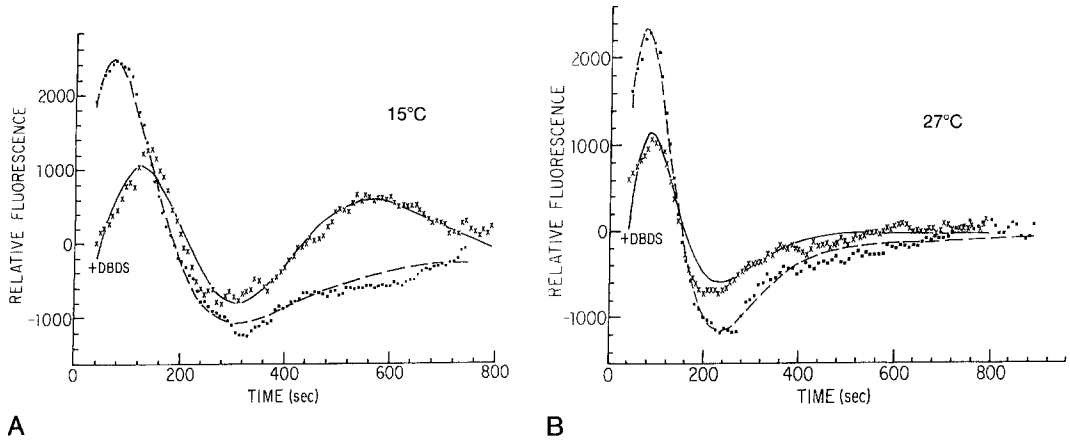

Fig. 10. Temperature dependence of 75 mM maltose induced tryptophan fluorescence. Red cells were incubated with DBDS (4 μM) in PBS for 10 min at 20–25°C and then equilibration at 15°C (*A*) or 27°C (*B*) before mixing with an equal volume of PBS (0 DBDS) in the stopped-flow apparatus. The baseline correction was measured for each blood at each temperature and the fitted $p(5)$ and $p(6)$ parameters were used to correct that data. The corrected data were then fitted by nonlinear least squares to the four parameters in Eq. (1). Average of five runs with two different bloods.

The fitted parameters are:

	$p(1)$ (fluorescence units)	$p(2)$ ($sec^{-1} \times 10^2$)	$p(3)$ ($sec^{-1} \times 10^1$)	$p(4)$ (sec)
15°C				
Control	3100 ± 90	0.32 ± 0.01	0.23 ± 0.01	5.0 ± 1.1
+ DBDS	1100 ± 100	0.13 ± 0.02	0.21 ± 0.01	49 ± 4
27°C				
Control	2900 ± 150	0.42 ± 0.01	0.33 ± 0.01	27.4 ± 0.7
+ DBDS	1400 ± 200	0.41 ± 0.01	0.34 ± 0.01	39.9 ± 0.7

frequency factor as 7.6 kcal mol^{-1} deg^{-1}. These activation energies may be compared with the values of $\Delta G^o = -8.5$ kcal mol^{-1} deg^{-1} for D-galactose binding to the arabinose binding protein in *E. coli* given by Quiocho (1986). Since Pimentel and McClellan (1960) estimate 3–5 kcal mol^{-1} deg^{-1} as the enthalpy of a single H-bond, the activation energies in Table 2 are consistent with restraints equivalent to about two H-bonds for each parameter, which seems not unreasonable for a system of disaccharide binding primarily dependent upon H-bonds.

Treatment with 2 μM DBDS causes a profound change in the oscillatory behavior following 75 mM maltose binding, as shown in Fig. 11*A*. As Table 2 reports, the activation energy of $p(2)$, the damping factor, increases by a factor of four to 38.9 ± 5.2 kcal mol^{-1} deg^{-1}, with little or no effect on $p(3)$. This increase in $p(2)$ shows quantitatively that the effect of DBDS on $p(2)$ is significant and, with Fig. 11*A*, confirms the conclusions that had already been reached on the basis of the more qualitative data in Table 1. Taken together with the previous findings of Janoshazi and Solomon (1989), there is clear evidence that information can travel in both directions through the linkage between band 3 and the glucose transport protein.

Our conclusions about the DBDS effect spring from our phenomenological observation of an oscillatory component in the tryptophan fluorescence following maltose binding. They are independent of the model that we have tentatively proposed as being consistent with the phenomenon. Our model is not unique and there can be any number of other models that can be invoked to account for the anharmonicity and the damping that characterize the data in Figs. 8 and 10, particularly in view of the complexity and depth of the cytoskeleton and the multiple relations between cytoskeletal and membrane elements. Our findings do show that the glucose transport proteins do not sit in the membrane like raisins in a cupcake, independent of the other proteins responsible for cell transport and membrane integrity. Indeed, the very sluggish time scale upon which the oscillations are played out is indicative of an extensive network

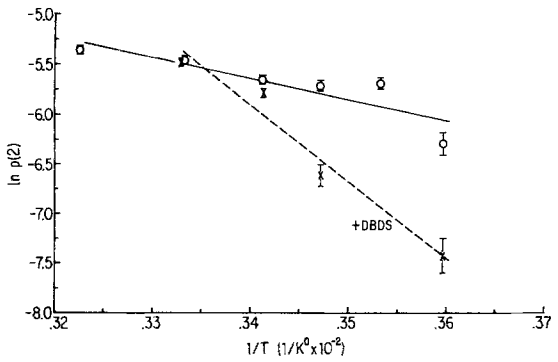

A

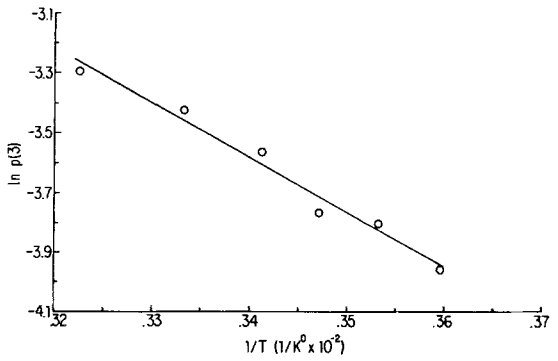

B

Fig. 11. Arrhenius plots (for blood 2) of the damping velocity parameter, $p(2)$ (*A*), and the angular frequency parameter, $p(3)$ (*B*; error bars are within the points). Experiments were carried out and the curves were fitted as described under Fig. 10. The parameters of the fit for blood 2 have been fitted to an exponential by nonlinear least squares to obtain the data in Table 2.

of elements whose interactions will eventually account for the phenomena we have observed.

This work was supported in part by a grant-in-aid from the American Heart Association, by the Squibb Institute for Medical Research and by The Council for Tobacco Research–U.S.A., Inc.

References

Alvarez, J., Lee, D.C., Baldwin, S.A., Chapman, C. 1987. Fourier transform infrared spectroscopic study of the structure and conformational changes in the human erythrocyte glucose transporter. *J. Biol. Chem.* **262:**3502–3509

Appleman, J.R., Lienhard, G.E. 1985. Rapid kinetics of the glucose transporter from human erythrocytes. *J. Biol. Chem.* **260:**4575–4578

Barnett, J.E.G., Holman, G.D., Chalkley, R.A., Munday, K.A. 1975. Evidence for two asymmetrical conformational states in the human erythrocyte sugar-transport system. *Biochem. J.* **145:**417–429

Barnett, J.E.G., Holman, G.D., Munday, K.A. 1973. An explanation of the asymmetric binding of sugars to the human erythrocyte sugar-transport systems. *Biochem. J.* **135:**539–541

Bennett, V., Stenbuck, P.J. 1980. Association between ankyrin and the cytoplasmic domain of band 3 isolated from the human erythrocyte membrane. *J. Biol. Chem.* **255:**6424–6432

Carruthers, A. 1986. Anomalous asymmetric kinetics of human red cell hexose transfer: Role of cytosolic adenosine 5'-triphosphate. *Biochemistry* **25:**3592–3602

Chance, B., Pye, E.K., Ghosh, A.K., Hess, B. (editors) 1973. Biological and Biochemical Oscillators. Academic, New York

Dix, J.A., Verkman, A.S., Solomon, A.K., Cantley, L.C. 1979. Human erythrocyte anion exchange site characterized using a fluorescent probe. *Nature* **282:**520–522

Duhm, V.J., Deuticke, B., Gerlach, E. 1969. Metabolism of 2,3-diphosphoglycerate and glycolysis in human erythrocytes. The influence of sulfate, tetrathionate and disulfite. *Hoppe-Seyler's Z. Physiol. Chem.* **350:**1008–1016

Fossel, E.T., Solomon, A.K. 1978. Ouabain-sensitive interaction between human red cell membrane and glycolytic enzyme complex in cytosol. *Biochim. Biophys. Acta* **510:**99–111

Gorga, F.R., Lienhard, G.E. 1982. Changes in the intrinsic fluorescence of the human erythrocyte monosaccharide transporter upon ligand binding. *Biochemistry* **21:**1905–1908

Helgerson, A.L., Carruthers, A. 1987. Equilibrium ligand binding to the human erythrocyte sugar transporter. *J. Biol. Chem.* **262:**5464–5475

Janoshazi, A., Solomon, A.K. 1989. Interaction among anion, cation and glucose transport proteins in the human red cell. *J. Membrane Biol.* **112:**25–37

Janoshazi, A., Solomon, A.K. 1990. Interaction between red cell glucose transport protein and band 3. *Biophys. J.* **57:**96*a*

Kahlenberg, A., Dolansky, D. 1972. Structural requirements of D-glucose for its binding to isolated human erythrocyte membranes. *Can. J. Biochem.* **50:**638–643

Kotaki, A., Naoi, M., Yagi, K. 1971. A diaminostilbene dye as a hydrophobic probe for proteins. *Biochim. Biophys. Acta* **224:**547–556

Krupka, R.M. 1971. Evidence for a carrier conformational change associated with sugar transport in erythrocytes. *Biochemistry* **10:**1143–1148

LeFevre, P.G. 1948. Evidence of active transfer of certain nonelectrolytes across the human red cell membrane. *J. Gen. Physiol.* **31:**505–527

Lew, V.L. 1971. On the ATP dependence of the Ca^{2+}-induced increase in K^+ permeability observed in human red cells. *Biochim. Biophys. Acta* **233:**827–830

May, J.M. 1987. Labelling of human erythrocyte band 3 with maltosylisothiocyanate. *J. Biol. Chem.* **262:**3140–3145

Miller, D.M., Olson, J.S., Pflugrath, J.W., Quiocho, F.A. 1983. Rates of ligand binding to periplasmic proteins involved in bacterial transport and chemotaxis. *J. Biol. Chem.* **258:**13665–13672

Mueckler, M. 1989. Structure and function of the glucose transporter. *In:* Red Blood Cell Membranes—Structure—Function—Clinical Implications. P. Agre and J.C. Parker, editors. pp: 31–45. Marcel Dekker, New York

Mueckler, M., Caruso, C., Baldwin, S.A., Panico, M., Blench, I., Morris, H.R., Allard, W.J., Lienhard, G.E., Lodish, H.F. 1985. Sequence and structure of a human glucose transporter. *Science* **229:**941–945

Mullins, R.E., Langdon, R.G. 1980*a*. Maltosyl isothiocyanate: An affinity label for the glucose transporter of the human erythrocyte membrane. 1. Inhibition of glucose transport. *Biochemistry* **19:**1199–1205

Mullins, R.E., Langdon, R.G. 1980*b*. Maltosyl isothiocyanate: An affinity label for the glucose transporter of the human

erythrocyte membrane. 2. Identification of the transporter. *Biochemistry* **19:**1205–1212

Pimentel, G.C., McClellan, A.L. 1960. The Hydrogen Bond. Table 7-II. Freeman, San Francisco

Quiocho, F.A. 1986. Carbohydrate-binding proteins: Tertiary structures and protein-sugar interactions. *Annu. Rev. Biochem.* **55:**287–315

Quiocho, F.A. 1989. Protein-carbohydrate interactions: Basic molecular features. *Pure Appl. Chem.* **61:**1293–1306

Rees, W.D., Gliemann, J., Holman, G.D. 1987. Re-examination of hexose-transporter inhibition and labelling by hexose isothiocyanates. *Biochem. J.* **241:**857–862

Rogalski, A.A., Steck, T.L., Waseem, A. 1989. Association of glyceraldehyde-3-phosphate dehydrogenase with the plasma membrane of the intact human red blood cell. *J. Biol. Chem.* **264:**6438–6446

Strapazon, E., Steck, T.L. 1977. Interaction of aldolase and the membrane of human erythrocytes. *Biochemistry* **16:**2966–2971

Verkman, A.S., Dix, J.A., Solomon, A.K. 1983. Anion transport inhibitor binding to band 3 in red blood cell membranes. *J. Gen. Physiol.* **81:**421–449

Verkman, A.S., Lukacovic, M.F., Tinklepaugh, M.S., Dix, J.A. 1986. Quenching of red cell tryptophan fluorescence by mercurial compounds. *Membrane Biochem.* **6:**269–289

Vyas, N.K., Vyas, M.N., Quiocho, F.A. 1988. Sugar and signal-transducer binding sites of the *Escherichia coli* galactose chemoreceptor protein. *Science* **242:**1290–1295

Walmsley, A.R. 1988. The dynamics of the glucose transporter. *Trends Biochem. Sci.* **13:**226–231

Widdas, W.F. 1988. Old and new concepts of the membrane transport for glucose in cells. *Biochim. Biophys. Acta* **947:**385–404

Yu, J., Steck, T.L. 1975. Associations of band 3, the predominant polypeptide of the human erythrocyte membrane. *J. Biol. Chem.* **250:**9176–9184

Received 4 September 1990; revised 8 April 1991

Appendix I

Disaccharide Structures from Merck Index

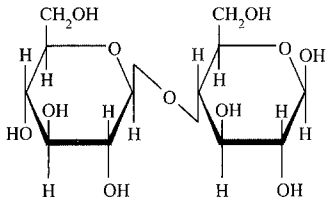

Cellobiose.

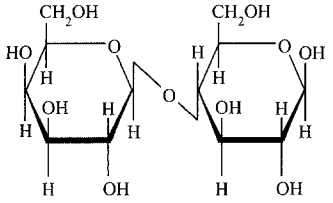

Lactose.

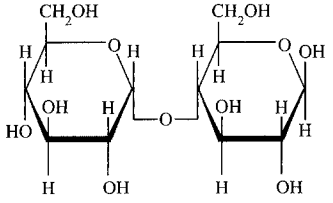

Maltose.

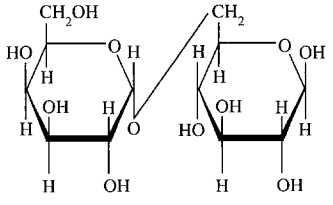

Melibiose.

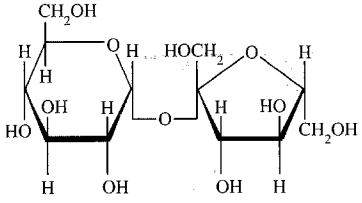

Sucrose.

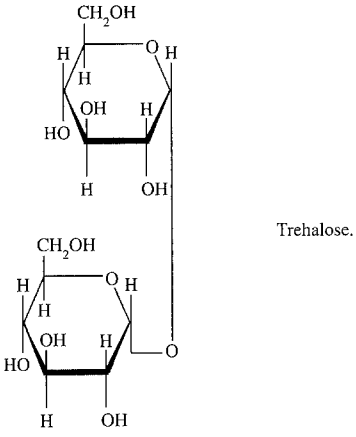

Trehalose.

Appendix II

We used a classical damped anharmonic oscillator model to see whether the results of our kinetic experiments could be analyzed in these terms. The equation of motion is given as

$$d^2y/dt^2 + A(dy/dt) + By^n = 0 \qquad \text{(A1)}$$

in which $A(dy/dt)$ is a resistive force, proportional to the velocity causing the damping. A has the dimension of frequency. In the

case of $n = 1$, the term, By^n, gives the harmonic oscillator equation, in which B represents the square of the angular frequency of the system in the absence of damping forces.

Since the frequency of the oscillations in our kinetic data, as shown in Figs. 8 and 10, decreases with time, we must choose a value of $n > 1$ to allow for the anharmonicity; we have chosen $n = 2$ for the weakest anharmonicity. Since there is no analytic solution for Eq. (A1) with $n = 2$, we have used the approximation

$$y(t) = C \exp(-At/2) \sin[(t/2)(4B \exp(-At/2) - A^2)^{1/2}] \quad \text{(A2)}$$

which is justified by the following considerations. If we solve Eq. (A1) with $n = 1$ in the form $y = \exp(\omega t)$ and substitute this relation in Eq. (A1), we obtain

$$(\omega^2 + A\omega + B)y = 0 \quad \text{(A3)}$$

which yields

$$\omega = (1/2)(-A \pm (A^2 - 4B)^{1/2}).$$

Using the identity

$$\exp(it) = \cos t + i \sin t.$$

If $4B > A^2$, the imaginary part of the solution is

$$y = \exp(-At/2) \sin[(t/2)(4B - A^2)^{1/2}].$$

The term A^2 will prove to be negligible as compared to $4B$, as will be seen from the fitting parameters, so we will use

$$y = \exp(-At/2) \sin[tB^{1/2}]. \quad \text{(A4)}$$

The approximate solution of Eq. (A1) with $n = 2$ can therefore be given by replacing B in Eq. (A3) by By which is approximated by $B \exp(-At/2)$. Using Eq. (A4), the approximate solution to Eq. (A1) with $n = 2$ is then given by

$$y(t) = C \exp(-At/2) \sin[tB^{1/2} \exp(-At/4)] \quad \text{(A5)}$$

which is a shorter form than Eq. (A2). If we assume that the oscillation starts at $t = t_o$, Eq. (A5) becomes

$$y(t) = C \exp(-A(t - t_o)/2) \sin\{(t - t_o)B^{1/2} \exp(-A(t - t_o)/4)\}. \quad \text{(A6)}$$

We define $p(1) \equiv C$; $p(2) \equiv -A/2$; $p(3) \equiv B^{1/2}$ and $p(4) \equiv t_o$. The results of the typical D-maltose experiment in Fig. 8*A* have not been corrected for the slow exponential baseline decay, whose time course is given by $[p(5) \exp(-p(6)t)]$. This additive term is superposed on the damped oscillation, so that the time course of the fluorescence signal in Fig. 8*A* is

$$y(t) = p(1) \exp[p(2)(t - p(4))] \sin\{(t - p(4))p(3) \exp[p(2)(t - p(4))/2]\} + p(5) \exp[-p(6)t]. \quad \text{(A7)}$$

The two parameters, $p(5)$ and $p(6)$ can be determined independently because they can be measured separately in a control experiment and stripped off from the rest of the equation since they enter Eq. (A7) only as the additive factor, $p(5) \exp[-p(6)t]$. Figure 8*B* shows the results of a control experiment in which the tryptophan fluorescence in red cells in PBS at room temperature was measured in the absence of D-maltose under the same conditions in which Fig. 8*A* was obtained in the presence of 75 mM D-maltose. The data in Fig. 8*B* have been fitted with an exponential with $p(5) = 0.29 \times 10^5$ fluorescence units and $p(6) = 0.19 \times 10^{-3}$ sec^{-1}. All six parameters in Fig. 8*A* have been determined by nonlinear least squares using a Microvax computer with the MAXSTAT program (IMS library) with the parameter values given in the legend. The fact that the six parameter fit gives values of $p(5) = 0.32 \times 10^5$ fluorescence units and $p(6) = 0.24 \times 10^{-3}$ sec^{-1} shows how closely the parameters in the control experiment fit the data. In view of this agreement, we determined $p(5)$ and $p(6)$ in a control experiment for each blood at each temperature and subtracted $p(5) \exp[-p(6)t]$ from the experimental data to make the appropriate baseline correction. After applying this procedure only four adjustable parameters remain to be determined to fit the data in these experiments. Figure 8*C* shows the data of Fig. 8*A* after the baseline correction and illustrates how well the four-parameter fitted curve fits the data. We have fitted the data for the set of experiments on the temperature dependence of the D-maltose effect (±DBDS) to the following four-parameter equation

$$y(t) = p(1) \exp[p(2)(t - p(4))] \sin\{(t - p(4))p(3) \exp[p(2)(t - p(4))/2]\}. \quad \text{(A8)}$$